

1
2
3 1 **An Ion Mobility and Gas-Phase Covalent Labeling Study of the**
4
5
6 2 **Structure and Reactivity of Gaseous Ubiquitin Ions Electro sprayed**
7
8
9 3 **from Aqueous and Denaturing Solutions**
10
11
12 4
13 5
14
15 6
16
17 7
18 8
19
20 9
21
22 10
23
24 11
25
26 12
27
28 13
29
30 14
31
32 15
33 16
34
35 17
36
37 18

38 19 Veronica V. Carvalho, Melanie Cheung See Kit, Ian K. Webb*

39
40 20 Indiana University Purdue University Indianapolis, Indianapolis, IN, USA 46202

41
42 21 * Correspondence to Ian K. Webb; e-mail: ikwebb@iu.edu
43
44 22
45
46 23

47 24 **Keywords:** Ion Mobility, native mass spectrometry, ion/ion reactions, covalent labeling
48
49 25
50
51 26
52
53 27
54
55 28

This is the author's manuscript of the article published in final edited form as:

Carvalho, V. V., See Kit, M. C., & Webb, I. K. (2020). Ion Mobility and Gas-Phase Covalent Labeling Study of the Structure and Reactivity of Gaseous Ubiquitin Ions Electro sprayed from Aqueous and Denaturing Solutions. *Journal of the American Society for Mass Spectrometry*. <https://doi.org/10.1021/jasms.9b00138>

1
2
3 29 **Abstract**
4

5 30 Gas-phase ion/ion chemistry was coupled to ion mobility/mass spectrometry analysis to
6
7 31 correlate the structure of gaseous ubiquitin to its solution structures with selective covalent
8
9 32 structural probes. Collision cross section (CCS) distributions were measured to ensure the
10
11 33 ubiquitin ions were not unfolded when they were introduced to the gas phase. Aqueous solutions
12
13 34 stabilizing the native state of ubiquitin yielded folded ubiquitin structures with CCS values
14
15 35 consistent with previously published literature. Denaturing solutions favored several families of
16
17 36 unfolded conformations for most of the charge states evaluated. Gas-phase covalent labeling via
18
19 37 ion/ion reactions was followed by collision induced dissociation of the intact, labeled protein to
20
21 38 determine which residues were labeled. Ubiquitin 5⁺ and 6⁺ electrosprayed from aqueous
22
23 39 conditions were covalently modified preferentially at the lysine 29 and arginine 54 positions,
24
25 40 indicating that elements of three-dimensional structure were maintained in the gas phase. On the
26
27 41 other hand, most ubiquitin ions produced in denaturing conditions were labeled at various other
28
29 42 lysine residues, likely due to the availability of additional sites following methanol and low pH-
30
31 43 induced unfolding. These data support the conservation of ubiquitin structural elements in the gas
32
33 44 phase. The research presented here provides the basis for residue-specific characterization of
34
35 45 biomolecules in the gas phase.
36
37
38
39 46
40
41
42
43
44
45
46
47
48
49
50
51
52
53
54
55
56
57
58
59
60

47 Introduction

48 Characterization of protein structures is critical for understanding their function.¹ The
49 development of “soft” ionization mass spectrometry in proteomics led to assays capable of
50 preserving non-covalent bonds as proteins transition from solution to the gas phase.²⁻³ Therefore,
51 a branch of biological mass spectrometry referred to as ‘native mass spectrometry’ (native MS)
52 has rapidly expanded, driven by the implicit hypothesis that specific interactions formed by
53 biomolecules in solution can be maintained under carefully controlled conditions for MS analysis
54 in the gas phase.⁴ Applications of native MS, ion mobility/mass spectrometry (IM/MS), and tandem
55 MS (MS/MS) involve probing proteins to obtain information such as higher order subunit
56 architecture, stoichiometry, shape, and sequence information.⁵⁻⁷

57 Ion/ion reaction chemistries have been exploited for analytical applications since the
58 beginning of the adoption of electrospray ionization (ESI), using mass spectrometers as the gas-
59 phase analog to the chemist’s wet bench.⁸⁻¹¹ The increasing use and versatility of ion/ion reactions
60 within the past half-decade has resulted from the development and commercial availability of
61 novel instrumentation equipped to perform such experiments.¹² Covalent labeling analyzed by
62 mass spectrometry (CLMS) is an example of a reaction that has been transferred from solution¹³⁻¹⁵
63 to the gas phase.¹⁶⁻¹⁹ Covalent modification by gas-phase ion/ion reactions relies on long-lived
64 complex formation between oppositely charged protein and reagent. In addition to containing an
65 electrostatically ‘sticky’ group (e.g., sulfonate or phosphate), reagents for covalent modification
66 require a reactive site that will undergo chemical reactions with the analyte ion. Several examples
67 of nucleophilic addition, utilizing electrophilic reagents such as reactive esters, have been
68 successfully applied.²⁰ Solution CLMS provides insight about protein conformations,²¹ dynamics,
69 and amino acid residue reactivity and microenvironment.²² CLMS, conducted in a tandem mass
70 spectrometer through ion/ion reactions, has the advantages of independent control/optimization
71 of reactant species, well-defined reaction conditions, reagent purification through mass-to-charge
72 isolation, and tandem MS capabilities in conjunction with ion/ion reactions.¹² Hence, ion/ion

1
2
3 73 covalent labeling coupled to IM-MS/MS can, in principle, provide for the three-dimensional
4
5 74 characterization of gaseous protein ions.²³⁻²⁴
6

7 75 Though most CLMS approaches have relied on 'bottom-up' proteomics, utilizing
8
9 76 enzymatic digestion to enable the identification of modification sites, the 'top-down' approach in
10
11 77 proteomics was developed in order to obtain primary structural information directly from the gas-
12
13 78 phase dissociation of intact protein ions without the need for extensive separations or digestion
14
15 79 prior to MS/MS analysis.²⁵ During a typical 'top-down' experiment, protein identification is made
16
17 80 by analyzing the sequence fragments of intact proteins from tandem MS, which allows for the
18
19 81 examination of the entire amino acid sequence, thereby characterizing intact proteins and
20
21 82 identifying the number and type of post-translational and other modifications in various so-called
22
23 83 proteoforms.²⁶
24
25

26 84 Solvent-free, gaseous proteins can maintain their solution structures with careful control
27
28 85 of experimental parameters.²⁷⁻²⁹ Pioneering studies from the laboratories of David Clemmer and
29
30 86 Michael Bowers revealed that ubiquitin solution structures can be preserved as kinetically trapped
31
32 87 intermediates in the gas phase after evaporative cooling associated with the electrospray
33
34 88 process. Their data suggested minor structural changes occur during desolvation of low charge
35
36 89 states ions ($z \cong 7$) for native-like conformations, and unfolded gas-phase structure happens for
37
38 90 higher charge states ($z \cong 13$) caused by rapid unfolding (<10 ms).³⁰ Additional studies evaluated
39
40 91 the abundance of different conformations of ubiquitin in the gas phase as a function of methanol
41
42 92 content in solution, where the native state was favored in aqueous solutions and more elongated
43
44 93 states of ubiquitin were dominant in solutions of 20:80 water:methanol content.³¹ The importance
45
46 94 in revealing the behavior and overall structure of native proteins in the gas phase is a
47
48 95 consequence of the increasing number of MS-related techniques applied in the field of structural
49
50 96 biology.³² Hence, it is essential to evaluate protein structures *in vacuo* after their transition from
51
52 97 solution into the gas phase with tools of higher structural specificity than ion mobility alone.
53
54
55
56
57
58
59
60

1
2
3 98 In this study, we focus on the three-dimensional characterization of gaseous protein ions
4
5 99 with CLMS performed completely inside the mass spectrometer. The structures of gaseous
6
7 100 ubiquitin generated from both aqueous and denaturing conditions were evaluated using ion/ion
8
9 101 chemistry, top-down tandem mass spectrometry, and ion mobility-derived collision cross section
10
11 102 measurements. Covalent labeling reactions between ubiquitin and sulfo-benzoyl-1-hydroxy-7-
12
13 103 azabenzotriazole ester (HOAt) were performed in the trap cell of a quadrupole IM-MS. The
14
15 104 reaction results in the formation of amide bonds with primary amines and guanidine in the gas-
16
17 105 phase. The protein ions are covalently modified by multiple additions of the reagent, separated
18
19 106 by ion mobility, and fragmented with mass analysis of the fragmentation products. Mass shifts in
20
21 107 the sequence fragments due to the covalent addition of the sulfo-benzoyl moiety allow for the
22
23 108 identification of covalently labeled sites. The results demonstrate the power of combining collision
24
25 109 cross section and covalent labeling approach to detect changes induced by solution conditions,
26
27 110 with measurements conducted entirely in the gas phase.
28
29
30
31 111

32 112 **Experimental**

33
34
35 113 **Materials.** Methanol, N,N-dimethyl formamide (DMF), and formic acid were purchased
36
37 114 from Fisher Scientific (Fairmont, NJ). Ubiquitin from bovine erythrocytes, myoglobin from horse
38
39 115 heart, cytochrome c from equine heart, and ammonium acetate were purchased from Sigma-
40
41 116 Aldrich (St. Louis, MO). 1-Hydroxy-7-azabenzonitrazole (HOAt) was purchased from TCI America
42
43 117 (Portland, OR). 1-Ethyl-3-(3-dimethylaminopropyl) carbodiimide hydrochloride (EDC) was
44
45 118 purchased from Thermo Scientific (Rockford, IL). 3-Sulfobenzoic acid monosodium salt was
46
47 119 purchased from Alfa Aesar (Ward Hill, MA).

48
49 120 **Sample Preparation.** For the experiments performed in denaturing conditions, ubiquitin
50
51 121 was dissolved in a 50/50/0.1 vol/vol solution of water/methanol/formic acid at 1 μ M. For analysis
52
53 122 using aqueous conditions, ubiquitin was dissolved in an aqueous 10 mM ammonium acetate
54
55 123 solution at 1 μ M. The reagent used for the ion/ion reactions, sulfo-benzoyl-HOAt, was synthesized

1
2
3 124 following a previously published procedure.³³ The calibrant mix used for CCS calculations
4
5 125 consisted of 1 μ M ubiquitin, cytochrome C, and myoglobin in 50:50:0.1 (v/v) solution of
6
7 126 water/methanol/formic acid.
8

9
10 127 **Traveling Wave Ion Mobility Spectrometry – CCS Calibration.** Calibration of drift time
11
12 128 measurements to known collision cross section values is necessary for traveling wave-type IM
13
14 129 instruments that use time-varying electric fields within the drift region. Traveling-wave drift times
15
16 130 were calibrated by measuring TWIMS profiles of a calibrant mix for each set of experiments
17
18 131 following a previously published protocol.³⁴⁻³⁶ A calibration curve (Fig. S3) was obtained by plotting
19
20 132 natural logarithm of the nitrogen CCS to charge ratios versus the calibrant ion drift times.³⁶ The
21
22 133 data was fit with a power function of the form given by Equation 1 where CCS_{N_2} is the calibrant
23
24 134 nitrogen CCS value, z is the charge state of the ion, and t_d is the drift time.
25

$$26 \quad 135 \quad \ln(CCS_{N_2}/z) = at_d^b \quad \text{Equation 1}$$

27
28
29 136 Nitrogen TWIMS CCS values were determined from measured drift times according to Equation
30
31 137 2.

$$32 \quad 138 \quad CCS = z * e^{at_d^b} \quad \text{Equation 2}$$

33
34
35 139 The CCS values were reported as the average obtained from triplicate measurements in Table
36
37 140 S1. The instrument settings used in CCS measurements and ion/ion reactions are summarized
38
39 141 in Table S2. All the CCS calibration calculations and results were reported as recommended by
40
41 142 recently introduced criteria.³⁷
42

43
44 143 **Mass Spectrometry and Ion/Ion Reactions.** Experiments were performed on a Synapt
45
46 144 G2-Si High Definition Mass Spectrometer (Waters Corporation, Wilmslow, U.K.) furnished with
47
48 145 electron transfer dissociation (ETD) and a NanoLockspray source. The instrumental arrangement
49
50 146 for the ion/ion reactions performed has been previously described.³⁸ Briefly, the source contains
51
52 147 two nanoelectrospray (nESI) probes positioned normal to each other and the sampling cone. The
53
54 148 nESI baffle was removed. Sequential anion (sulfobenzoyl-HOAt) and cation (ubiquitin) ionization
55
56
57
58
59
60

1
2
3 149 was enabled by a WRENS (Waters Research Enabled Software) script coupled with ETD mode
4
5 150 to synchronize ion injection with the polarity of the instrument optics and ETD refill times (1s each)
6
7 151 for reagent and cation fills, respectively. Infusion flow rates were 500 nl/min or lower.
8

9 152 The control sequence consists of injecting ions through the stepwave region with m/z
10
11 153 isolation in the quadrupole. Anions are trapped in the trap cell in the first step, followed by
12
13 154 introduction of a specific analyte (cationic) charge state (again, m/z isolated by the quadrupole)
14
15 155 into the trap. Next, reaction products are pulsed out of the trap, separated by their mobilities, and
16
17 156 then traverse the transfer cell where the transfer collision energy is increased allowing for collision
18
19 157 induced dissociation after the reaction products exit the mobility cell. Thus, ion/ion reactions
20
21 158 products and their sequence fragments share identical drift times since fragments were not
22
23 159 generated until after IM separation. Ions were mass analyzed by the time-of-flight mass
24
25 160 spectrometer in Resolution Mode (nominal resolving power of 20,000 FWHM). Tandem mass
26
27 161 spectra were internally calibrated against the monoisotopic mass of the y_{18}^{2+} fragment ion from
28
29 162 ubiquitin (m/z 1049.0997).
30
31

32 163 **Data Analysis.** Mobility-selected mass spectra were extracted with the instrument control
33
34 164 software MassLynx V4. Extracted mass spectra were converted into .mgf (Mascot Generic
35
36 165 Format) files and imported into Mash Explorer,³⁹ where spectra were deconvoluted by the
37
38 166 eThrash algorithm⁴⁰ with a S/N threshold of 3, peak background ratio of 1, peptide minimum
39
40 167 background ratio of 1, and minimum isotopic fit % of 80. The covalently modified and unmodified
41
42 168 CID fragments obtained for all experiments were investigated against the ubiquitin primary
43
44 169 sequence by applying custom PTMs equal to the mass of the covalent modification formed by the
45
46 170 ion/ion reactions (i.e., 182.98 Da) at the N and C termini. Covalently modified peaks were
47
48 171 annotated with a mass error tolerance of 20 ppm.⁴¹ The annotations were then manually
49
50 172 confirmed.
51
52

53 173
54
55
56 174
57
58
59
60

175 **Results and Discussion**

176 **Protein Mass Spectra.** The ions produced by nESI ionization of ubiquitin from both
177 aqueous and denaturing conditions exhibit characteristic distributions (Fig. S1) when analyzed
178 with the “softest” conditions that allowed enough ion transmission to collect mass and mobility
179 spectra (Table S2). A profile of high m/z signals with lower charge states (i.e., $6 \geq z \geq 4$) peaks
180 for ubiquitin was observed for the sample sprayed from aqueous conditions. A distribution of
181 higher charge state peaks ($13 \geq z \geq 5$) with considerably higher relative intensities was obtained
182 using denaturing conditions. The charge state distributions suggest that ubiquitin ions
183 electrosprayed under aqueous conditions have a compact solution structure, as supported by the
184 literature.^{32, 42} The compact native state of ubiquitin has a limited number of amino acid residues
185 accessible for protonation. On the other hand, the higher charge states exhibited for denaturing
186 conditions are evidence of the disruption of the tertiary structure of ubiquitin.⁴³⁻⁴⁵ The observed
187 transition in charge state distributions indicates that methanol induces structural transitions for
188 ubiquitin.

189 **Gas-Phase Ubiquitin Conformations in the Trap Cell from Native and Denaturing**
190 **Conditions.** To compare ubiquitin conformations generated from different solution conditions,
191 calibrated collision cross sections were measured for each of the charge states that was
192 investigated by covalent labeling with both denaturing and aqueous conditions (Table S1). The
193 experimental conditions applied for CCS calibration and ion/ion reactions were identical (with
194 exception of the gas flows into the helium and mobility cells) and are summarized in Table S2.
195 Ubiquitin conformers originating from aqueous and denaturing conditions were assessed by
196 converting the peaks in the ion mobility arrival time distributions (ATDs) to CCS values, allowing
197 for the characterization of ubiquitin populations that undergo ion/ion reaction chemistry. Thus, we
198 are chiefly concerned with the ion populations present in the trap cell prior to the ion mobility
199 separation, as these are the populations directly probed by the ion/ion reactions. Therefore, we

1
2
3 200 minimized the trap and mobility voltages to prevent unintended activation. The %CV values for
4
5 201 the calibrated CCS values measured on three different days were less than 2.5%. Figures 1A and
6
7 202 1B show the ATDs for ubiquitin 5⁺ and 6⁺ in aqueous and denaturing conditions. In solution,
8
9 203 aqueous conditions of ubiquitin favor the N-state (native state) while the partially unfolded so-
10
11 204 called A-state is dominant in solutions containing 40% methanol or more.⁴⁶⁻⁴⁸ Ions generated from
12
13 205 aqueous conditions presented a narrow structural region with similar cross section values
14
15 206 ($^{TW}CCSN_2$ – 1193 Å² and 1233 Å², for ubiquitin 5⁺ and 6⁺, respectively) corresponding to compact
16
17 207 conformations.⁴⁹ For aqueous ubiquitin 6⁺ a minor peak is present at ~1371 Å², which is likely
18
19 208 composed of partially folded states. Previous reports of the 6⁺ charge state generated from
20
21 209 solutions of ubiquitin in aqueous ammonium acetate with ATDs measured by both drift tube and
22
23 210 TWIMS instruments also display this feature.^{34, 50} The presence of these states is best explained
24
25 211 by the increase in Coulombic repulsion from the additional proton bound to the 6⁺ charge state
26
27 212 versus the 5⁺, as the 5⁺ charge state lacks this more extended feature.³¹ Similarly, the distribution
28
29 213 for ubiquitin 5⁺ in denaturing conditions (Fig. 1) displays a distribution of compact ions (~1228 Å²)
30
31 214 that extends into the region corresponding to partially folded ions (~1333 Å²). Ubiquitin 6⁺ in
32
33 215 denaturing conditions gives a broad distribution (from ~1300 Å² to 1900 Å²) that can be related to
34
35 216 multiple stable, elongated forms. Although this distribution is broad, there are 2 features with
36
37 217 maxima at ~1398 Å² and ~1676 Å², corresponding to a partially unfolded intermediate state and
38
39 218 partially unfolded structure arising from the A state, respectively. Figure S2 presents the CCS
40
41 219 distributions for all charge states of electrosprayed ubiquitin ions from aqueous and denaturing
42
43 220 solutions. The distributions for ubiquitin 7⁺ and 8⁺ prepared in denaturing conditions are dominated
44
45 221 by relatively sharper features at ~1834 Å² and ~1906 Å², respectively. Sharper features in protein
46
47 222 ATDs indicate that the ion conformer population is collapsed into relatively few stable structures
48
49 223 that exist over a narrow region of the available cross section space and appear as a result of
50
51 224 protein unfolding.⁵⁰
52
53
54
55
56 225

226 **Characterization of Gaseous Ubiquitin Structures with Ion/Ion Reactions.**

227 *Covalent modification of ubiquitin via ion/ion reaction in the gas phase.* Covalent bond
228 formation occurs via ion/ion reactions by a three-step process: 1) Formation of a stable, long-lived
229 electrostatically bound complex; 2) Activation of the complex; and 3) Dissociation of the leaving
230 group from the complex. The first step is completed by trapping both reagent anions and protein
231 cations in the trap cell. A minimal amplitude trap traveling wave (< 0.2 V) is used to promote better
232 mixing and, in effect, increases the effective reaction time.⁵¹ The product is observed by a shift in
233 m/z equal to a reduction in charge by the number of reagents electrostatically attached and an
234 increase in mass equal to the molecular mass of the reagent. Next, the complex is activated. The
235 pressures and voltages from the source and into the trap cell were kept identical to the conditions
236 used for our CCS measurements to prevent gas-phase unfolding prior to the ion/ion reaction.
237 Thus, the protein ions that were labeled structurally correlate with the observed arrival time
238 distributions and CCS values. The transition state for a covalent reaction between a model amine
239 and sulfobenzoyl-HOAt has been calculated to be 17.4 kcal/mol higher in energy than the
240 electrostatic product.³³ The sulfonate is expected to be electrostatically attached to a protonated
241 arginine, lysine, or histidine residue. The proton transfer barrier for transfer from guanidinium to
242 sulfonate was calculated to be 61 kcal/mol and for transfer from ammonium to sulfonate was
243 calculated to be 28 kcal/mol higher in energy than the complex. Since collisional activation on a
244 mass spectrometry timescale is kinetically controlled, enough collisional energy must be applied
245 to form the covalent reaction transition state but not high enough to result in proton transfer without
246 covalent bond formation or fragmentation of the protein.

247 Though the application of this energy may lead to coulombically-driven unfolding of the
248 protein, the strong electrostatic “anchor” holds the reagent in place. The through-bond distance
249 from the reactive carbonyl carbon to the sulfonate oxygens in the reagent is approximately 6.4 Å.
250 Thus, the reactive side chain must be close by the charged anchoring residue (i.e., on the surface
251 of the protein) and a reactive nucleophile. Therefore, though collision-induced unfolding or

1
2
3 252 intramolecular proton transfer may occur during the activation of the complex, these processes
4
5 253 are not expected to affect the ability of the ion/ion reaction to report on surface accessible regions
6
7 254 of the protein that are nearby external, protonated side chains. The fact that the reagent to
8
9 255 protonated side chain noncovalent bond is not fragmented under these conditions illustrates that
10
11 256 the applied activation to form the covalent product is mild. The applied collisional energy will drive
12
13 257 off the weakly-bound leaving group after the covalent product is formed. The covalent reaction is
14
15 258 observed by a decrease in m/z equal to neutral loss of the leaving group.

16
17
18 259 Ion/ion reactions were used to probe the gas phase microenvironment and relative
19
20 260 reactivity of lysine and arginine side chains in ubiquitin cations formed from the aqueous and
21
22 261 denaturing solutions. Previously, histidine was found to only react with low energy activation
23
24 262 applied over long time periods.³³ These conditions cannot be accessed with the instrument used
25
26 263 in this study as CID is performed in transmission mode (beam-type CID). Therefore, we do not
27
28 264 expect to observe histidine modification. Ion/ion reactions were performed under similar ion optics
29
30 265 voltage conditions as the CCS measurements from the source up to and including the trap cell
31
32 266 (*vide supra*). The choice of the sulfobenzoyl-HOAt reagent (versus, e.g., sulfobenzoyl-N-
33
34 267 hydroxysuccinimide) was based on its relatively low activation energy for covalent reactions in
35
36 268 the gas phase, its simple and one-pot synthesis, and the ability of sulfo-benzoyl-HOAt to react
37
38 269 with amino acids side chains such as arginine and lysine.³³

39
40
41 270 Figure 2A displays the ion/ion reaction of ubiquitin 6⁺ electrosprayed from aqueous
42
43 271 conditions and sulfobenzoyl-HOAt. The amide bond formation between ubiquitin and 3-
44
45 272 sulfobenzoate is characterized by the neutral loss of HOAt (Molecular mass = 135.1235 g/mol)
46
47 273 from the ion/ion reaction product. The peak $[M+6H+\blacklozenge]^{5+}$ represents the electrostatic product
48
49 274 formed between ubiquitin 6⁺ and the reagent, $[M+5H+*]^{5+}$ is covalently modified ubiquitin, and the
50
51 275 $[M + 5H]^{5+}$ peak is the proton transfer product corresponding to the loss of the electrostatically
52
53 276 attached reagent. In order to favor covalent product formation (as opposed to proton transfer)
54
55 277 several parameters were optimized aiming to apply energy below the threshold for proton transfer
56
57
58
59
60

1
2
3 278 product formation but above the transition state energy for covalent bond formation.⁵² With the
4
5 279 helium cell and IM pressures used to measure CCS, the only observed product upon collisional
6
7 280 activation was loss of the reagent from the ion/ion product complex. This is due to intentional rapid
8
9 281 thermalization of ions by many low-energy collisions as they enter the mobility cell, preventing
10
11 282 unintended activation of ions.⁵³ However, rapid thermalization results in the need to use much
12
13 283 higher voltages to achieve ion activation, with the consequence of not being able to access the
14
15 284 neutral loss of HOAt channel, as the loss of the entire reagent is kinetically favorable. Previous
16
17 285 work has shown that the transition state for loss of an electrostatically bound reagent is very loose
18
19 286 compared the transition state for covalent reaction,⁵⁴ restraining the appearance of the covalent
20
21 287 reaction to activation energies below the threshold for loss of the entire reagent. Therefore, the
22
23 288 gas flows into the helium and IM cells were set to 20 mL/min each (0.59 and 0.66 mbar pressures
24
25 289 for each of the cells, respectively). This way, the injection energy into the mobility cell was able to
26
27 290 be reduced (center of mass energy of 3.6 kcal/mol for 5⁺, Table S4) and fewer energizing
28
29 291 collisions occur. The result is efficient formation of the -HOAt without a dominant channel for loss
30
31 292 of the entire reagent. The tune parameters used during ion/ion reactions are presented in Table
32
33 293 S2. The trap pressure was kept the same. In this way, the ratio of the covalently modified product
34
35 294 to the proton transfer (reagent loss) peak was maximized to yield the mass spectrum in Figure
36
37 295 2A.³⁸ The ATD in Figure 2B was obtained under these conditions and represents the ion mobility
38
39 296 separation of different numbers of sequential ion/ion reactions between ubiquitin 6⁺ and sulfo-
40
41 297 benzoyl-HOAt. The peak at 65 ms is related to the precursor ubiquitin 6⁺, the peak at ~78 ms
42
43 298 corresponds to the attachment of one sulfobenzoyl-HOAt, and the peaks at ~96 and 120 ms
44
45 299 correspond to attachment of two and three sulfobenzoyl-HOAt, respectively. Figure 2C displays
46
47 300 the mass spectrum at extracted from drift time 72 – 83 ms resulting from CID of the ion/ion reaction
48
49 301 covalent modified product. Figure 3 shows the mass spectra related to the peaks in the ATD which
50
51 302 correspond to the ion/ion reactions products obtained for ubiquitin 7⁺ in denaturing conditions,
52
53 303 with up to three covalent additions of sulfobenzoyl-HOAt reagents. Fragments from CID of the
54
55
56
57
58
59
60

1
2
3 304 labeled protein ions were only investigated for addition of a single label to help prevent label-
4
5 305 induced structural changes from affecting our analysis.¹⁵
6

7 306 The charge states 5⁺ and 6⁺ ionized from aqueous conditions and 5⁺, 6⁺, 7⁺, and 8⁺ all
8
9 307 displayed a neutral loss of m/z 136 (the mass of the leaving group, HOAT) following ion/ion
10
11 308 reactions with sulfobenzoyl-HOAt. However, 7⁺ and 8⁺ from aqueous conditions and 9⁺ from
12
13 309 denaturing conditions did not show neutral loss of HOAt. The only products were the electrostatic
14
15 310 addition of sulfobenzoyl-HOAt and loss of the entire reagent. This observation is attributed to the
16
17 311 lack of unprotonated lysine or arginine residues available on the exterior of the protein with 7⁺ and
18
19 312 8⁺ ionized from aqueous conditions and 9⁺ ionized from denaturing conditions. The difference in
20
21 313 reactivity between the 7⁺ and 8⁺ charge states ionized from aqueous solution and 7⁺ and 8⁺ from
22
23 314 denaturing solution indicate that their protonation sites and gas-phase structures are likely
24
25 315 different. The injection energy was controlled to prevent fragmentation of the protein backbone.
26
27 316 No fragments other than the loss of HOAt or the entire reagent were observed without adding
28
29 317 collisional energy in the transfer cell.
30
31

32 318 *Comparison and characterization of the ubiquitin ion structures obtained from aqueous*
33
34 319 *and denaturing solutions.* CID was performed upon injection into the transfer cell to form covalent
35
36 320 modification sequence fragments originating from different charge states of ubiquitin in both
37
38 321 aqueous (ubiquitin 5⁺ and 6⁺) and denaturing (ubiquitin 5⁺ to 8⁺) conditions. Table S3 summarizes
39
40 322 the collision energy voltages applied to the transfer cell for each CID experiment. The covalent
41
42 323 product ions generated *b* (N-terminal) and *y* (C-terminal) fragment ions that matched drift times
43
44 324 of their precursors. Figure 2C shows the fragment mass spectrum resulting from CID of the
45
46 325 covalent product $[M+5H+*]^{5+}$ that was used to determine the sites of covalent modification. The
47
48 326 fragment ion annotations from the solution condition and charge state-dependent ion/ion gas-
49
50 327 phase covalent modification of ubiquitin are shown in Tables 1 and 2.
51
52

53 328 For ubiquitin 5⁺ and 6⁺ electrosprayed from aqueous conditions the modified fragment ions
54
55 329 generated suggested covalent modifications to lysine 29 (modified b_{29}) and arginine 54 (modified
56
57
58
59
60

1
2
3 330 y_{24}) which is in agreement with previously published work.³⁸ The residues available for covalent
4
5 331 modification must be accessible to the reagent – which excludes side chains buried in the interior
6
7 332 of the protein – and reactive towards the reagent, precluding protonated and non-nucleophilic
8
9 333 sites. Modification sites were annotated based on the smallest terminal (b- or y-ion) fragment that
10
11 334 has a m/z shift corresponding to covalent addition. The process of assigning labeled sites is as
12
13 335 follows: b- and y-ions that matched the m/z of sequence fragments plus the mass of the covalent
14
15 336 label were annotated as covalently labeled fragments and manually validated. Next, the mass
16
17 337 spectra were manually compared against spectra resulting from CID of unmodified ubiquitin at
18
19 338 the same charge. Fragments that were originally annotated as covalently labeled that matched
20
21 339 the m/z and isotopic distribution of fragments resulting from CID of unmodified ubiquitin were
22
23 340 thrown out and considered false positives. Side chains were assigned as covalently labeled only
24
25 341 if there was no evidence for covalent labeling of amino acid residues N-terminal (for b-ions) or C-
26
27 342 terminal (for y-ions) to the assigned site (i.e., no labeled sequence fragments that include these
28
29 343 residues). For example, Table 1 shows that the smallest labeled b-ion was modified b_{29} , but
30
31 344 unmodified fragments are observed for b_{27} and b_{28} , ions that include the N-terminus, K6, K11, and
32
33 345 K27, but not K29. Therefore, there is no evidence for labeling of any of these amino acids, but the
34
35 346 observation of b-ions matching the mass of the addition of the covalent label that include K29
36
37 347 suggests that K29 is the labeled side chain. These results correlate to the crystal structure of
38
39 348 ubiquitin (PDB 1UBQ)⁵⁵ where the suggested modified residues are exposed and accessible to
40
41 349 the reagent (Figure 4). Recently, results from 193 nm ultraviolet photodissociation (UVPD) were
42
43 350 used to determine the protonation sites for different native charge states of ubiquitin in the gas
44
45 351 phase.⁵⁶ The possible protonation sites for the 5^+ and 6^+ charge state were determined to be Q2,
46
47 352 P19, K33, R42, K48, K63, and R74. For both charge states, K29 and R54 are not protonated,
48
49 353 rendering them reactive to sulfobenzoyl-HOAt. The solvent-accessible surface area (SASA) was
50
51 354 calculated from the crystal structure with a probe size of 1.4 Å (i.e., the van der Waals radius of
52
53 355 water) with the GETAREA program.⁵⁷ Side chains with a SASA ratio above 30% were considered

1
2
3 356 solvent accessible.⁵⁸ Including the accessible arginine and lysine side chains from the SASA
4
5 357 calculation and excluding the UVPD-determined protonated side chains limits the remaining
6
7 358 available sites for labeling by sulfobenzoyl-HOAt to K6, K11, K29, R54, and R72, although K11
8
9 359 (and K27) participates in a salt bridge and thus may not be labeled if these salt bridges are not
10
11 360 disrupted under our labeling conditions.⁵⁹ The observed labeling of K29 and R54 (Fig. 4) suggests
12
13 361 that ubiquitin structures electrosprayed from aqueous conditions retain elements of solution
14
15 362 structure, as predicted by molecular dynamics⁶⁰ and the structure relaxation approximation⁶⁰⁻⁶¹.
16
17
18 363 K27 is not labeled, although it is only two residues away from K29, and is also not protonated.
19
20 364 This may be evidence that elements of solution structure can be maintained, as K27 and K29 are
21
22 365 in an alpha helix. Although the side chain of K27 faces the interior of the protein, the alpha helix
23
24 366 positions K29 to be oriented outwards.⁵⁵ Another interpretation of these results could suggest that
25
26 367 the label is electrostatically bound to a side chain that is greater than 6.4 Å from the primary amine
27
28 368 of the K27 side chain. Nonetheless, the labeling of K29 and K27 is not random (it occurs
29
30 369 repeatably for both 5⁺ and 6⁺ charge states electrosprayed from aqueous solution) and does
31
32 370 correlate with the region of the protein including K29 being accessible. The combination of CCS
33
34 371 data, mass spectra, identified covalently modified residues, and modeling for native ubiquitin 5⁺
35
36 372 and 6⁺ suggests that ubiquitin structures remain compact in the gas phase when electrosprayed
37
38 373 from aqueous conditions.⁶⁰

39
40
41 374 Ubiquitin has been shown to undergo an alcohol-induced transition to a partially folded
42
43 375 state (A state). For the A state, NMR experiments performed in a 40:60 water:methanol solution
44
45 376 suggested that it retains a majority of its native secondary structural elements in the N-terminal
46
47 377 half, whereas the structure of the C-terminal half unfolds to a highly helical more elongated
48
49 378 state.^{31, 62-64} For the 5⁺ ion sprayed from a denaturing solution, our ion/ion reaction results show
50
51 379 that K29 and R54 are labeled (Table 2), the same results as determined for the 5⁺ ions from
52
53 380 aqueous conditions, consistent with CCS distribution being very similar between the 5⁺ sprayed
54
55 381 from denaturing conditions and the 5⁺ and 6⁺ sprayed from native conditions. The ion/ion covalent

1
2
3 382 labeling also illustrates that the peak around 1400 Å in the aqueous 6⁺ and denaturing 5⁺ likely
4
5 383 reflects compact structures, since the labeled sites are identical for native 5⁺/6⁺ and denaturing
6
7 384 5⁺. This is consistent with molecular dynamics data that show reversible unfolding and folding for
8
9 385 ubiquitin 6⁺ ions generated from native conditions for 1 μs in the gas phase.⁶⁰ Additionally, the 6⁺
10
11 386 and 7⁺ charge state fragments include modified y₂₄, also indicating that R54 was labeled. The
12
13 387 labeling of R54 under various conditions indicates that for charge states 5⁺-7⁺, R54 is
14
15 388 unprotonated, accessible, and sufficiently reactive under all these conditions.

16
17
18 389 However, the 6⁺, 7⁺, and 8⁺ charge states of ubiquitin sprayed from denaturing solution
19
20 390 were all labeled at different lysine residues, with no evidence for labeling at the K29 residue. As
21
22 391 previously illustrated, these ions all produced ATDs showing more extended conformations. This
23
24 392 suggests that K29 is no longer the most reactive accessible lysine side chain for these charge
25
26 393 states. The 6⁺ fragmentation data shows that K48 is likely labeled (modified b₅₂), the 7⁺
27
28 394 fragmentation data shows labeling likely occurs on K33 (modified b₃₆), and the 8⁺ data may provide
29
30 395 evidence for the labeling of K27, though the lack of labeled b-ions for the 8⁺ charge state gives
31
32 396 some ambiguity to this assignment. The reduced number of labeled sequence fragments for the
33
34 397 8⁺ ions is likely a consequence of most of the reactive residues in ubiquitin being protonated,
35
36 398 diminishing the overall reactivity and the number of available sites for labeling. The labeling of 6⁺
37
38 399 at K48 and 7⁺ at K33 is likely due to changes in preferred protonation sites following the unfolding
39
40 400 of the protein, as are K33 and K48 can both be protonated when sprayed from aqueous
41
42 401 conditions. NMR measurements have demonstrated that a characteristic of the A-state is that the
43
44 402 solution salt bridge between K27 and D52, which stabilizes the fold of the protein and buries K27
45
46 403 in the interior of the protein, is disrupted.⁶³⁻⁶⁴ Therefore, our results for 6⁺ and 7⁺ ionized from
47
48 404 denaturing conditions correlate with at least partially disrupted solution states. Covalent labeling
49
50 405 by ion/ion reactions is expected to be a powerful tool for protein structural analysis.

51
52
53
54 406
55
56 407

408 Conclusions

409 Ubiquitin ions electrosprayed from aqueous and denaturing solutions have been analyzed
410 by IM-MS/MS and covalent structural probes delivered by ion/ion reactions inside of the mass
411 spectrometer. Ubiquitin conformational populations were evaluated prior to performing ion/ion
412 reactions by IM-MS, ensuring that energy imparted on the ions between the source and trap cell
413 did not lead to collision induced unfolding. Examination of the conformation types as function of
414 the solution conditions and charge states allowed for solution structures to be correlated to gas-
415 phase measurements, suggesting the preservation of solution-like structures in the gas phase.
416 Ions generated from aqueous solution had CCS values corresponding to compact conformations
417 while ubiquitin 6⁺ also exhibited a minor peak at ~1371 Å², which has been attributed to partially
418 folded states due to the increase in Coulombic repulsion over the 5⁺ charge state. On the other
419 hand, arrival time distributions for ubiquitin in denaturing conditions presented much higher CCS
420 values which have been previously correlated to multiple elongated stable conformations.^{44-45, 65}

421 The covalent modification data revealed distinct characteristics for ions originating from
422 either aqueous or denaturing conditions. For aqueous conditions, the modified fragment ions
423 suggested covalent modifications to lysine 29 (modified b₃₂) and arginine 54 (modified y₂₄). It is
424 possible that elements of secondary structure as well as tertiary structure are conserved
425 explained by the covalent modification of K29 instead of the buried and salt-bridged K27.⁵¹⁻⁵²
426 These results correlate to the crystal structure of ubiquitin (PDB 1UBQ)⁵⁵, molecular dynamics
427 results⁵⁷, and UVPD data,⁴⁸ where the modified residues are exposed and accessible to the
428 reagent. Ion/ion reaction results for ubiquitin 5⁺ sprayed from denaturing solutions also reveal the
429 labeling of K29 and R54, agreeing with the CCS data, and suggesting that aqueous 6⁺ and
430 denaturing 5⁺ are structurally very similar. Therefore, the denaturing 5⁺ ion is produced from the
431 remaining compact ubiquitin population in denaturing solutions. The 6⁺, 7⁺, and 8⁺ charge states
432 of ubiquitin sprayed from denaturing solutions were labeled at various lysines, accessible most
433 likely due to the changes in possible protonation sites as a result disruption of the salt bridge

1
2
3 434 between K27 and D52 after methanol-induced unfolding.⁵⁵⁻⁵⁶ Overall, the analysis of protein
4
5 435 structures by covalent modification in the gas phase analyzed by IM-MS/MS suggests that the
6
7 436 gas phase is a suitable environment for probing protein structure if care is taken to ensure gentle
8
9 437 ion introduction.

10 438

11 12 13 439 **Acknowledgement**

14
15 440 Portions of this work were funded by the National Institutes of Health (NIH) NIGMS Grant R21
16
17 441 GM134408 (I.K.W.). The authors would like to acknowledge Lindsay Morrison and Jeffery
18
19 442 Brown of Waters Corporation for helpful discussions.

20 443

21 22 23 444 **Associated Content**

24
25 445 Supporting Information

26
27 446 Ubiquitin electrospray mass spectra, CCS of ubiquitin charge states from aqueous and
28
29 447 denaturing solutions, ion/ion product spectra, annotated sequence ions from CID of covalently
30
31 448 modified ubiquitin, tabulated CCS values, experimental parameters, and ion energies used
32
33 449 during covalent modification.

34 450

451 **References**

- 452 1. Ishima, R.; Torchia, D. A., Protein dynamics from NMR. *Nat Struct Biol* **2000**, 7 (9), 740-
453 3.
- 454 2. Loo, J. A.; Loo, R. R. O.; Udseth, H. R.; Edmonds, C. G.; Smith, R. D., Solvent-Induced
455 Conformational-Changes of Polypeptides Probed by Electrospray-Ionization Mass-
456 Spectrometry. *Rapid Commun Mass Sp* **1991**, 5 (3), 101-105.
- 457 3. Chowdhury, S. K.; Katta, V.; Chait, B. T., An electrospray-ionization mass spectrometer
458 with new features. *Rapid Commun Mass Spectrom* **1990**, 4 (3), 81-7.
- 459 4. Ishii, K.; Zhou, M.; Uchiyama, S., Native mass spectrometry for understanding dynamic
460 protein complex. *Biochim Biophys Acta Gen Subj* **2018**, 1862 (2), 275-286.
- 461 5. Lanucara, F.; Holman, S. W.; Gray, C. J.; Eyers, C. E., The power of ion mobility-mass
462 spectrometry for structural characterization and the study of conformational dynamics. *Nat*
463 *Chem* **2014**, 6 (4), 281-294.
- 464 6. Resing, K. A.; Ahn, N. G., Proteomics strategies for protein identification. *FEBS Letters*
465 **2005**, 579 (4), 885-889.
- 466 7. Konijnenberg, A.; Butterer, A.; Sobott, F., Native ion mobility-mass spectrometry and
467 related methods in structural biology. *Biochim. Biophys. Acta* **2013**, 1834 (6), 1239-1256.
- 468 8. Loo, R. R. O.; Udseth, H. R.; Smith, R. D., Evidence of charge inversion in the reaction
469 of singly charged anions with multiply charged macroions. *The Journal of Physical Chemistry*
470 **1991**, 95 (17), 6412-6415.
- 471 9. Ogorzalek Loo, R. R.; Udseth, H. R.; Smith, R. D., A new approach for the study of gas-
472 phase ion-ion reactions using electrospray ionization. *J Am Soc Mass Spectrom* **1992**, 3 (7),
473 695-705.
- 474 10. Herron, W. J.; Goeringer, D. E.; McLuckey, S. A., Product Ion Charge State
475 Determination via Ion/Ion Proton Transfer Reactions. *Anal Chem* **1996**, 68 (2), 257-262.
- 476 11. Stephenson, J. L.; McLuckey, S. A., Simplification of Product Ion Spectra Derived from
477 Multiply Charged Parent Ions via Ion/Ion Chemistry. *Anal Chem* **1998**, 70 (17), 3533-3544.
- 478 12. Foreman, D. J.; McLuckey, S. A., Recent Developments in Gas-Phase Ion/Ion Reactions
479 for Analytical Mass Spectrometry. *Anal Chem* **2019**.
- 480 13. Oetjen, J.; Rexroth, S.; Reinhold-Hurek, B., Mass spectrometric characterization of the
481 covalent modification of the nitrogenase Fe-protein in *Azoarcus* sp. BH72. *The FEBS Journal*
482 **2009**, 276 (13), 3618-3627.
- 483 14. Guan, J.-Q.; Chance, M. R., Structural proteomics of macromolecular assemblies using
484 oxidative footprinting and mass spectrometry. *Trends in Biochemical Sciences* **2005**, 30 (10),
485 583-592.
- 486 15. Mendoza, V. L.; Vachet, R. W., Probing protein structure by amino acid-specific covalent
487 labeling and mass spectrometry. *Mass Spectrom. Rev.* **2009**, 28 (5), 785-815.
- 488 16. Peng, Z.; McLuckey, S. A., C-terminal peptide extension via gas-phase ion/ion reactions.
489 *International Journal of Mass Spectrometry* **2015**, 391, 17-23.
- 490 17. McGee, W. M.; McLuckey, S. A., Efficient and directed peptide bond formation in the gas
491 phase via ion/ion reactions. *Proceedings of the National Academy of Sciences* **2014**, 111 (4),
492 1288.
- 493 18. Prentice, B. M.; McGee, W. M.; Stutzman, J. R.; McLuckey, S. A., Strategies for the gas
494 phase modification of cationized arginine via ion/ion reactions. *International Journal of Mass*
495 *Spectrometry* **2013**, 354-355, 211-218.
- 496 19. Mentinova, M.; McLuckey, S. A., Covalent Modification of Gaseous Peptide Ions with N-
497 Hydroxysuccinimide Ester Reagent Ions. *J Am Chem Soc* **2010**, 132 (51), 18248-18257.
- 498 20. Prentice, B. M.; McLuckey, S. A., Gas-phase ion/ion reactions of peptides and proteins:
499 acid/base, redox, and covalent chemistries. *Chem. Commun.* **2013**, 49 (10), 947-965.

- 1
2
3 500 21. Loo, J. A.; Loo, R. R. O.; Goodlett, D. R.; Smith, R. D.; Fuciarelli, A. F.; Springer, D. L.;
4 501 Thrall, B. D.; Edmonds, C. G., Elucidation of Covalent Modifications and Noncovalent
5 502 Associations in Proteins by Electrospray Ionization Mass Spectrometry. In *Techniques in*
6 503 *Protein Chemistry IV*, Angeletti, R. H., Ed. Academic Press: 1993; pp 23-31.
- 7 504 22. Limpikirati, P.; Pan, X.; Vachet, R. W., Covalent Labeling with Diethylpyrocarbonate:
8 505 Sensitive to the Residue Microenvironment, Providing Improved Analysis of Protein Higher
9 506 Order Structure by Mass Spectrometry. *Anal. Chem.* **2019**, *91* (13), 8516-8523.
- 10 507 23. Webb, I. K.; Mentinova, M.; McGee, W. M.; McLuckey, S. A., Gas-phase intramolecular
11 508 protein crosslinking via ion/ion reactions: ubiquitin and a homobifunctional sulfo-NHS ester. *J.*
12 509 *Am. Soc. Mass. Spectrom.* **2013**, *24* (5), 733-43.
- 13 510 24. Pitts-McCoy, A. M.; Harrilal, C. P.; McLuckey, S. A., Gas-Phase Ion/Ion Chemistry as a
14 511 Probe for the Presence of Carboxylate Groups in Polypeptide Cations. *J. Am. Soc. Mass.*
15 512 *Spectrom.* **2019**, *30* (2), 329-338.
- 16 513 25. Reid, G. E.; McLuckey, S. A., 'Top down' protein characterization via tandem mass
17 514 spectrometry. *J Mass Spectrom* **2002**, *37* (7), 663-75.
- 18 515 26. Smith, L. M.; Kelleher, N. L.; Linial, M.; Goodlett, D.; Langridge-Smith, P.; Ah Goo, Y.;
19 516 Safford, G.; Bonilla*, L.; Kruppa, G.; Zubarev, R.; Rontree, J.; Chamot-Rooke, J.; Garavelli, J.;
20 517 Heck, A.; Loo, J.; Penque, D.; Hornshaw, M.; Hendrickson, C.; Pasa-Tolic, L.; Borchers, C.;
21 518 Chan, D.; Young*, N.; Agar, J.; Masselon, C.; Gross*, M.; McLafferty, F.; Tsybin, Y.; Ge, Y.;
22 519 Sanders*, I.; Langridge, J.; Whitelegge*, J.; Marshall, A.; The Consortium for Top Down, P.,
23 520 Proteoform: a single term describing protein complexity. *Nat. Methods* **2013**, *10* (3), 186-187.
- 24 521 27. Ruotolo, B. T.; Giles, K.; Campuzano, I.; Sandercock, A. M.; Bateman, R. H.; Robinson,
25 522 C. V., Evidence for Macromolecular Protein Rings in the Absence of Bulk Water. *Science* **2005**,
26 523 *310* (5754), 1658.
- 27 524 28. Skinner, O. S.; McLafferty, F. W.; Breuker, K. J. J. o. t. A. S. f. M. S., How ubiquitin
28 525 unfolds after transfer into the gas phase. **2012**, *23* (6), 1011-1014.
- 29 526 29. Loo, J. A.; He, J. X.; Cody, W. L. J. J. o. t. A. C. S., Higher order structure in the gas
30 527 phase reflects solution structure. **1998**, *120* (18), 4542-4543.
- 31 528 30. Wyttenbach, T.; Bowers, M. T., Structural Stability from Solution to the Gas Phase:
32 529 Native Solution Structure of Ubiquitin Survives Analysis in a Solvent-Free Ion Mobility–Mass
33 530 Spectrometry Environment. *The Journal of Physical Chemistry B* **2011**, *115* (42), 12266-12275.
- 34 531 31. Shi, H. L.; Clemmer, D. E., Evidence for Two New Solution States of Ubiquitin by IMS-
35 532 MS Analysis. *J Phys Chem B* **2014**, *118* (13), 3498-3506.
- 36 533 32. Ruotolo, B. T.; Robinson, C. V., Aspects of native proteins are retained in vacuum. *Curr.*
37 534 *Opin. Chem. Biol.* **2006**, *10* (5), 402-408.
- 38 535 33. Bu, J.; Peng, Z.; Zhao, F.; McLuckey, S. A., Enhanced Reactivity in Nucleophilic Acyl
39 536 Substitution Ion/Ion Reactions Using Triazole-Ester Reagents. *J. Am. Soc. Mass. Spectrom.*
40 537 **2017**, *28* (7), 1254-1261.
- 41 538 34. Sun, Y.; Vahidi, S.; Sowole, M. A.; Konermann, L. J. J. o. T. A. S. f. M. S., Protein
42 539 Structural Studies by Traveling Wave Ion Mobility Spectrometry: A Critical Look at Electrospray
43 540 Sources and Calibration Issues. **2016**, *27* (1), 31-40.
- 44 541 35. Ruotolo, B. T.; Benesch, J. L.; Sandercock, A. M.; Hyung, S.-J.; Robinson, C. V. J. N. p.,
45 542 Ion mobility–mass spectrometry analysis of large protein complexes. **2008**, *3* (7), 1139.
- 46 543 36. Bush, M. F.; Hall, Z.; Giles, K.; Hoyes, J.; Robinson, C. V.; Ruotolo, B. T., Collision
47 544 Cross Sections of Proteins and Their Complexes: A Calibration Framework and Database for
48 545 Gas-Phase Structural Biology. *Anal. Chem.* **2010**, *82* (22), 9557-9565.
- 49 546 37. Gabelica, V.; Shvartsburg, A. A.; Afonso, C.; Barran, P.; Benesch, J. L.; Bleiholder, C.;
50 547 Bowers, M. T.; Bilbao, A.; Bush, M. F.; Campbell, J. L. J. M. s. r., Recommendations for
51 548 reporting ion mobility mass spectrometry measurements. **2019**.

- 1
2
3 549 38. Webb, I. K.; Morrison, L. J.; Brown, J. J. I. J. o. M. S., Dueling electrospray implemented
4 550 on a traveling-wave ion mobility/time-of-flight mass spectrometer: Towards a gas-phase
5 551 workbench for structural biology. **2019**, *444*, 116177.
- 6 552 39. Cai, W.; Guner, H.; Gregorich, Z. R.; Chen, A. J.; Ayaz-Guner, S.; Peng, Y.; Valeja, S.
7 553 G.; Liu, X.; Ge, Y., MASH Suite Pro: A Comprehensive Software Tool for Top-Down Proteomics.
8 554 *Mol. Cell. Proteomics* **2016**, *15* (2), 703-14.
- 9 555 40. Horn, D. M.; Zubarev, R. A.; McLafferty, F. W., Automated reduction and interpretation
10 556 of. *J. Am. Soc. Mass. Spectrom.* **2000**, *11* (4), 320-332.
- 11 557 41. Donnelly, D. P.; Rawlins, C. M.; DeHart, C. J.; Fornelli, L.; Schachner, L. F.; Lin, Z.;
12 558 Lippens, J. L.; Aluri, K. C.; Sarin, R.; Chen, B.; Lantz, C.; Jung, W.; Johnson, K. R.; Koller, A.;
13 559 Wolff, J. J.; Campuzano, I. D. G.; Auclair, J. R.; Ivanov, A. R.; Whitelegge, J. P.; Paša-Tolić, L.;
14 560 Chamot-Rooke, J.; Danis, P. O.; Smith, L. M.; Tsybin, Y. O.; Loo, J. A.; Ge, Y.; Kelleher, N. L.;
15 561 Agar, J. N., Best practices and benchmarks for intact protein analysis for top-down mass
16 562 spectrometry. *Nat. Methods* **2019**, *16* (7), 587-594.
- 17 563 42. Wyttenbach, T.; Bowers, M. T., Structural stability from solution to the gas phase: native
18 564 solution structure of ubiquitin survives analysis in a solvent-free ion mobility-mass spectrometry
19 565 environment. *J. Phys. Chem. B* **2011**, *115* (42), 12266-75.
- 20 566 43. Konermann, L.; Douglas, D. J., Unfolding of proteins monitored by electrospray
21 567 ionization mass spectrometry: a comparison of positive and negative ion modes. *J. Am. Soc.*
22 568 *Mass. Spectrom.* **1998**, *9* (12), 1248-1254.
- 23 569 44. Shi, H.; Pierson, N. A.; Valentine, S. J.; Clemmer, D. E., Conformation Types of Ubiquitin
24 570 [M+8H]⁸⁺ Ions from Water:Methanol Solutions: Evidence for the N and A States in Aqueous
25 571 Solution. *The Journal of Physical Chemistry B* **2012**, *116* (10), 3344-3352.
- 26 572 45. Shi, H.; Clemmer, D. E., Evidence for two new solution states of ubiquitin by IMS-MS
27 573 analysis. *The journal of physical chemistry. B* **2014**, *118* (13), 3498-3506.
- 28 574 46. Brutscher, B.; Brüschweiler, R.; Ernst, R. R. J. B., Backbone dynamics and structural
29 575 characterization of the partially folded A state of ubiquitin by ¹H, ¹³C, and ¹⁵N nuclear
30 576 magnetic resonance spectroscopy. **1997**, *36* (42), 13043-13053.
- 31 577 47. Lenkinski, R. E.; Chen, D. M.; Glickson, J. D.; Goldstein, G. J. B. e. B. A.-P. S., Nuclear
32 578 magnetic resonance studies of the denaturation of ubiquitin. **1977**, *494* (1), 126-130.
- 33 579 48. Wilkinson, K. D.; Mayer, A. N. J. A. o. b.; biophysics, Alcohol-induced conformational
34 580 changes of ubiquitin. **1986**, *250* (2), 390-399.
- 35 581 49. May, J. C.; Jurneczko, E.; Stow, S. M.; Kratochvil, I.; Kalkhof, S.; McLean, J. A.,
36 582 Conformational Landscapes of Ubiquitin, Cytochrome c, and Myoglobin: Uniform Field Ion
37 583 Mobility Measurements in Helium and Nitrogen Drift Gas. *Int J Mass Spectrom* **2018**, *427*, 79-
38 584 90.
- 39 585 50. May, J. C.; Jurneczko, E.; Stow, S. M.; Kratochvil, I.; Kalkhof, S.; McLean, J. A.,
40 586 Conformational landscapes of ubiquitin, cytochrome c, and myoglobin: Uniform field ion mobility
41 587 measurements in helium and nitrogen drift gas. *Int. J. Mass spectrom.* **2018**, *427*, 79-90.
- 42 588 51. Lermyte, F.; Verschuere, T.; Brown, J. M.; Williams, J. P.; Valkenburg, D.; Sobott, F.,
43 589 Characterization of top-down ETD in a travelling-wave ion guide. *Methods* **2015**, *89*, 22-29.
- 44 590 52. Bu, J.; Fisher, C. M.; Gilbert, J. D.; Prentice, B. M.; McLuckey, S. A. J. J. o. T. A. S. f. M.
45 591 S., Selective covalent chemistry via gas-phase ion/ion reactions: an exploration of the energy
46 592 surfaces associated with N-hydroxysuccinimide ester reagents and primary amines and
47 593 guanidine groups. **2016**, *27* (6), 1089-1098.
- 48 594 53. Giles, K.; Williams, J. P.; Campuzano, I., Enhancements in travelling wave ion mobility
49 595 resolution. *Rapid Commun. Mass Spectrom.* **2011**, *25* (11), 1559-1566.
- 50 596 54. Bu, J.; Fisher, C. M.; Gilbert, J. D.; Prentice, B. M.; McLuckey, S. A., Selective Covalent
51 597 Chemistry via Gas-Phase Ion/ion Reactions: An Exploration of the Energy Surfaces Associated
52 598 with N-Hydroxysuccinimide Ester Reagents and Primary Amines and Guanidine Groups. *J. Am.*
53 599 *Soc. Mass. Spectrom.* **2016**, *27* (6), 1089-1098.

- 1
2
3 600 55. Vijaykumar, S.; Bugg, C. E.; Cook, W. J., Structure of Ubiquitin Refined at 1.8 a
4 601 Resolution. *J Mol Biol* **1987**, *194* (3), 531-544.
- 5 602 56. Morrison, L. J.; Brodbelt, J. S., Charge site assignment in native proteins by ultraviolet
6 603 photodissociation (UVPD) mass spectrometry. *Analyst* **2016**, *141* (1), 166-176.
- 7 604 57. Fraczkiwicz, R.; Braun, W., Exact and efficient analytical calculation of the accessible
8 605 surface areas and their gradients for macromolecules. *J. Comput. Chem.* **1998**, *19* (3), 319-333.
- 9 606 58. Mendoza, V. L.; Vachet, R. W., Protein Surface Mapping Using Diethylpyrocarbonate
10 607 with Mass Spectrometric Detection. *Anal. Chem.* **2008**, *80* (8), 2895-2904.
- 11 608 59. Harding, M. M.; Williams, D. H.; Woolfson, D. N., Characterization of a Partially
12 609 Denatured State of a Protein by 2-Dimensional Nmr - Reduction of the Hydrophobic Interactions
13 610 in Ubiquitin. *Biochemistry* **1991**, *30* (12), 3120-3128.
- 14 611 60. Bakhtiari, M.; Konermann, L., Protein Ions Generated by Native Electrospray Ionization:
15 612 Comparison of Gas Phase, Solution, and Crystal Structures. *The Journal of Physical Chemistry*
16 613 *B* **2019**, *123* (8), 1784-1796.
- 17 614 61. Bleiholder, C.; Liu, F. C., Structure Relaxation Approximation (SRA) for Elucidation of
18 615 Protein Structures from Ion Mobility Measurements. *The Journal of Physical Chemistry B* **2019**,
19 616 *123* (13), 2756-2769.
- 20 617 62. Cox, M. J.; Haas, A. L.; Wilkinson, K. D., Role of ubiquitin conformations in the specificity
21 618 of protein degradation: iodinated derivatives with altered conformations and activities. *Arch*
22 619 *Biochem Biophys* **1986**, *250* (2), 400-9.
- 23 620 63. Pan, Y. Q.; Briggs, M. S., Hydrogen-Exchange in Native and Alcohol Forms of Ubiquitin.
24 621 *Biochemistry-Us* **1992**, *31* (46), 11405-11412.
- 25 622 64. Stockman, B. J.; Euvrard, A.; Scahill, T. A., Heteronuclear three-dimensional NMR
26 623 spectroscopy of a partially denatured protein: the A-state of human ubiquitin. *J Biomol NMR*
27 624 **1993**, *3* (3), 285-96.
- 28 625 65. Shi, H.; Atlasevich, N.; Merenbloom, S. I.; Clemmer, D. E., Solution Dependence of the
29 626 Collisional Activation of Ubiquitin [M + 7H]⁷⁺ Ions. *J. Am. Soc. Mass. Spectrom.* **2014**, *25* (12),
30 627 2000-2008.

628

629

630

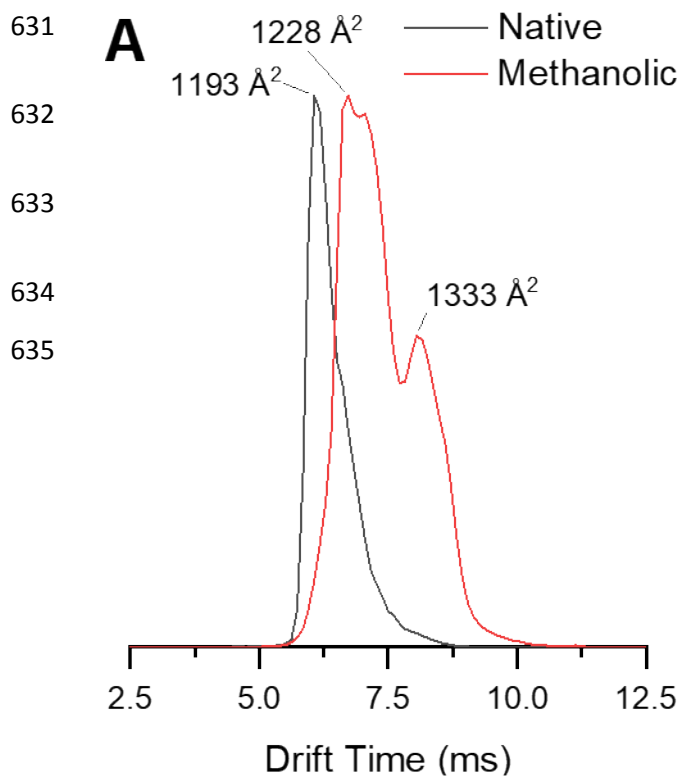
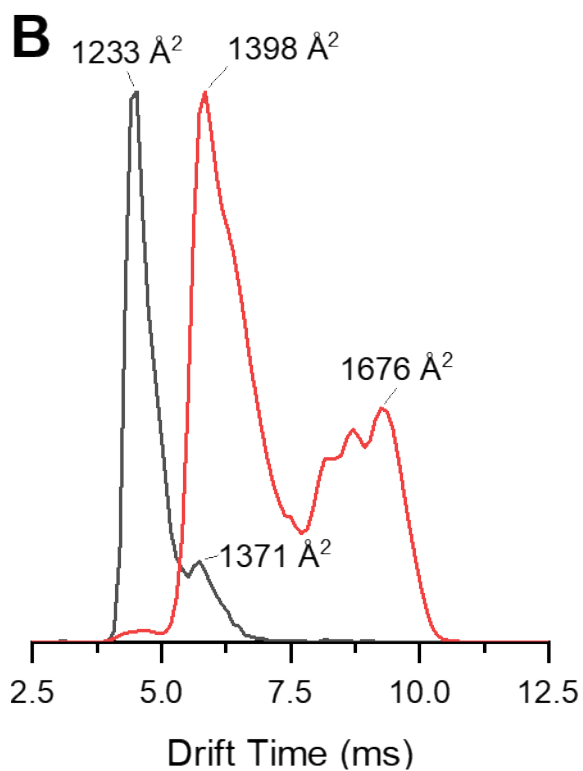
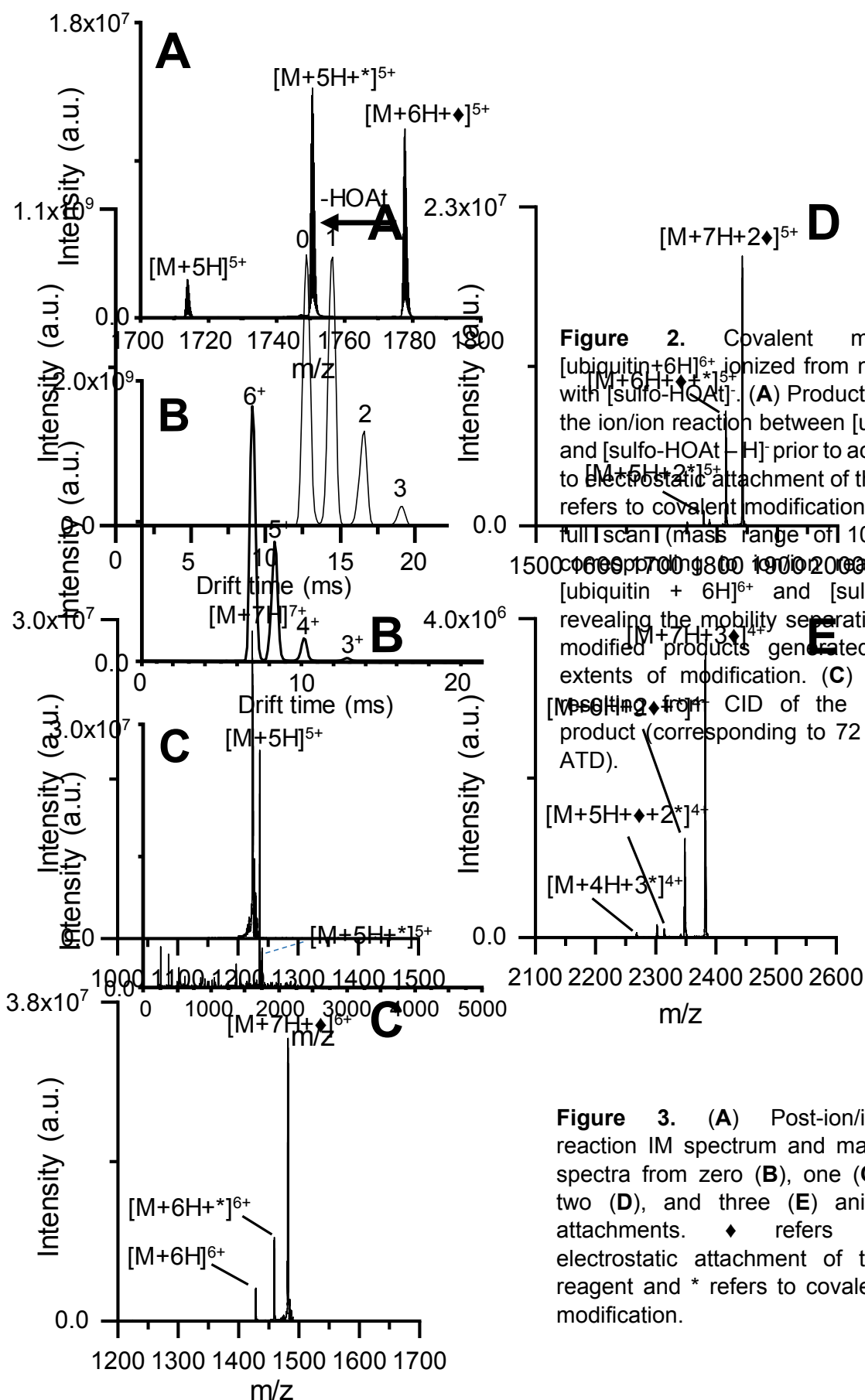
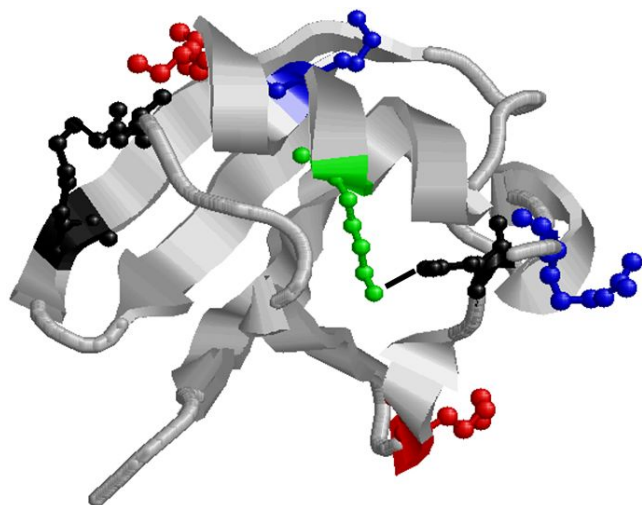


Figure 1. Intensity normalized arrival time distributions (ATDs) of ubiquitin 5⁺ (**A**) and 6⁺ (**B**) charge states sprayed from native (black trace) and denaturing (red trace) conditions.







639

640 **Figure 4.** X-ray structure of ubiquitin (1ubq). The blue residues (K29, R54) are labeled under
641 native conditions and the red (K33, K48) and green residue (K27) are labeled only under
642 denaturing conditions. The red residues are protonated under native conditions and the green
643 residue is buried and participates in a salt bridge with D52 (black). K11 is black as it participates
644 in a salt bridge but is not labeled under any conditions. The black line between K27 and D52
645 represents the salt bridge.

646

647 **Table 1.** Sequence Ladder for Aqueous Ubiquitin in different charge states displaying the
 648 covalently modified fragmentation sites and the modified residues.

	Charge state	Sequence ladder for Ubiquitin																																																																											
		1	10	20	30	40	50	60	70																																																																				
Aqueous Modified	[M+5H] ⁵⁺	M	Q	I	F	V	K	T	L	T	G	K	T	I	T	L	E	V	E	P	S	D	T	I	E	N	V	K	A	K	I	Q	D	K	E	G	I	P	P	D	Q	Q	R	L	I	F	A	G	K	Q	L	E	D	G	R	T	L	S	D	Y	N	I	Q	K	E	S	T	L	H	L	V	L	R	L	R	G	G
	[M+6H] ⁶⁺	M	Q	I	F	V	K	T	L	T	G	K	T	I	T	L	E	V	E	P	S	D	T	I	E	N	V	K	A	K	I	Q	D	K	E	G	I	P	P	D	Q	Q	R	L	I	F	A	G	K	Q	L	E	D	G	R	T	L	S	D	Y	N	I	Q	K	E	S	T	L	H	L	V	L	R	L	R	G	G
	[M+7H] ⁷⁺	No modification identified, facile loss of reagent																																																																											
	[M+8H] ⁸⁺	No modification identified, facile loss of reagent																																																																											
Aqueous Unmodified	[M+5H] ⁵⁺	M	Q	I	F	V	K	T	L	T	G	K	T	I	T	L	E	V	E	P	S	D	T	I	E	N	V	K	A	K	I	Q	D	K	E	G	I	P	P	D	Q	Q	R	L	I	F	A	G	K	Q	L	E	D	G	R	T	L	S	D	Y	N	I	Q	K	E	S	T	L	H	L	V	L	R	L	R	G	G
	[M+6H] ⁶⁺	M	Q	I	F	V	K	T	L	T	G	K	T	I	T	L	E	V	E	P	S	D	T	I	E	N	V	K	A	K	I	Q	D	K	E	G	I	P	P	D	Q	Q	R	L	I	F	A	G	K	Q	L	E	D	G	R	T	L	S	D	Y	N	I	Q	K	E	S	T	L	H	L	V	L	R	L	R	G	G

649

650

651

652

653

654

655

656

657 **Table 2.** Sequence Ladder for Denatured Ubiquitin in different charge states displaying the
 658 covalently modified fragmentation sites and the modified residues.

	Charge state	Sequence ladder for Ubiquitin																																																																											
		1	10	20	30	40	50	60	70																																																																				
Denatured Modified	[M+5H] ⁵⁺	M	Q	I	F	V	K	T	L	T	G	K	T	I	T	L	E	V	E	P	S	D	T	I	E	N	V	K	A	K	I	Q	D	K	E	G	I	P	P	D	Q	Q	R	L	I	F	A	G	K	Q	L	E	D	G	R	T	L	S	D	Y	N	I	Q	K	E	S	T	L	H	L	V	L	R	L	R	G	G
	[M+6H] ⁶⁺	M	Q	I	F	V	K	T	L	T	G	K	T	I	T	L	E	V	E	P	S	D	T	I	E	N	V	K	A	K	I	Q	D	K	E	G	I	P	P	D	Q	Q	R	L	I	F	A	G	K	Q	L	E	D	G	R	T	L	S	D	Y	N	I	Q	K	E	S	T	L	H	L	V	L	R	L	R	G	G
	[M+7H] ⁷⁺	M	Q	I	F	V	K	T	L	T	G	K	T	I	T	L	E	V	E	P	S	D	T	I	E	N	V	K	A	K	I	Q	D	K	E	G	I	P	P	D	Q	Q	R	L	I	F	A	G	K	Q	L	E	D	G	R	T	L	S	D	Y	N	I	Q	K	E	S	T	L	H	L	V	L	R	L	R	G	G
	[M+8H] ⁸⁺	M	Q	I	F	V	K	T	L	T	G	K	T	I	T	L	E	V	E	P	S	D	T	I	E	N	V	K	A	K	I	Q	D	K	E	G	I	P	P	D	Q	Q	R	L	I	F	A	G	K	Q	L	E	D	G	R	T	L	S	D	Y	N	I	Q	K	E	S	T	L	H	L	V	L	R	L	R	G	G
	[M+9H] ⁹⁺	No modification identified, facile loss of reagent																																																																											
Denatured Unmodified	[M+5H] ⁵⁺	M	Q	I	F	V	K	T	L	T	G	K	T	I	T	L	E	V	E	P	S	D	T	I	E	N	V	K	A	K	I	Q	D	K	E	G	I	P	P	D	Q	Q	R	L	I	F	A	G	K	Q	L	E	D	G	R	T	L	S	D	Y	N	I	Q	K	E	S	T	L	H	L	V	L	R	L	R	G	G
	[M+6H] ⁶⁺	M	Q	I	F	V	K	T	L	T	G	K	T	I	T	L	E	V	E	P	S	D	T	I	E	N	V	K	A	K	I	Q	D	K	E	G	I	P	P	D	Q	Q	R	L	I	F	A	G	K	Q	L	E	D	G	R	T	L	S	D	Y	N	I	Q	K	E	S	T	L	H	L	V	L	R	L	R	G	G
	[M+7H] ⁷⁺	M	Q	I	F	V	K	T	L	T	G	K	T	I	T	L	E	V	E	P	S	D	T	I	E	N	V	K	A	K	I	Q	D	K	E	G	I	P	P	D	Q	Q	R	L	I	F	A	G	K	Q	L	E	D	G	R	T	L	S	D	Y	N	I	Q	K	E	S	T	L	H	L	V	L	R	L	R	G	G
	[M+8H] ⁸⁺	M	Q	I	F	V	K	T	L	T	G	K	T	I	T	L	E	V	E	P	S	D	T	I	E	N	V	K	A	K	I	Q	D	K	E	G	I	P	P	D	Q	Q	R	L	I	F	A	G	K	Q	L	E	D	G	R	T	L	S	D	Y	N	I	Q	K	E	S	T	L	H	L	V	L	R	L	R	G	G

659

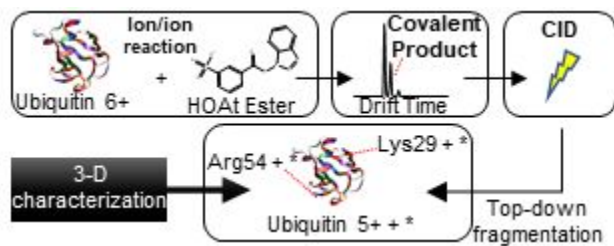
660

661

662

663

664

665 **Graphical Abstract**

666

667 Caption: A gas-phase ion/ion reaction covalent modification and ion mobility/mass spectrometry
668 workflow for determining three-dimensional structural information.

669

670

671

672

673

674

675

676

677

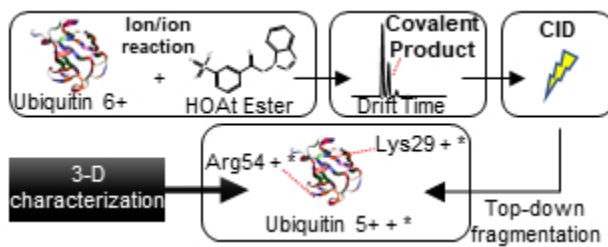
678

679

680

681

682



A gas-phase ion/ion reaction covalent modification and ion mobility/mass spectrometry workflow for determining three-dimensional structural information.

82x31mm (96 x 96 DPI)